Generation of Synthetic Earthquake Accelerograms based on up-to-date Seismological Ground Motion Models

Yuxiang Tang[1], Nelson Lam[1], Elisa Lumantarna[1], Hing Ho Tsang[2]

1. Corresponding Author, Department of Infrastructural Engineering, The University of Melbourne, Parkville, VIC 3010, Australia. Email: tangyuxiang56@gmail.com

   Associate Professor and Reader, Department of Infrastructural Engineering, The University of Melbourne, Parkville, VIC 3010, Australia. Email: ntkl@unimelb.edu.au

   Lecturer, Department of Infrastructural Engineering, The University of Melbourne, Parkville, VIC 3010, Australia. Email: elu@unimelb.edu.au

2. Lecturer, Faculty of Science, Engineering and Technology, Swinburne University of Technology, Melbourne, VIC 3122, Australia. Email: htsang@swin.edu.au

Abstract

This paper aims at introducing to structural or geotechnical engineering designers and researchers over the use of synthetic accelerograms as a supplement to recorded accelerograms for input into time-history analysis of structural systems. The computational algorithm for stochastic simulations of the seismological model for generation of accelerograms is presented to enable readers to generate accelerograms by *MATLAB*, or *EXCEL*, instead of proprietary software (avoiding the *black box* syndrome). A listing of seismological models that have been developed by reputable sources is provided. As shown in the paper a seismological model can be evaluated, and compared, with other ground motion models through *probabilistic seismic hazard analysis* (PSHA). A comparison of predictions from ground motion models proposed for use in *Eastern North America* (NGA – East) with predictions from the *Next Generation Attenuation relationships* for *Western North America* (NGA-West2) is presented in the concluding sections of the paper.

Keywords: synthetic accelerograms, stochastic simulations, seismological models, response spectrum

1. Introduction

Accelerograms are required whenever non-linear time history analyses are involved in the design of a structure, or in researching into its performance behaviour. To operate those analyses multiple records for every projected earthquake scenarios (M-R combinations) would be required to cover for random inter-event variability. Although codes of practices typically require only 3 - 7 accelerograms to be incorporated into time history analyses a much higher number of accelerograms would be necessary to provide a robust indication of trends characterising the seismic response behaviour of a structure. The *Pacific Earthquake Engineering Research Centre* (PEER) database contains thousands of strong motion accelerograms but only those recorded from a M4.5 - M7 event are of engineering interests in Australia. Consider the case where the structure to be designed is founded on a soil site. Selecting a recording station at which the subsoil conditions match with the geology of the site which the structure is founded upon can be difficult. Programs such as *SHAKE* can be used to simulate ground motions on the soil surface provided that the subsoil model (showing relevant details of each soil layer) is known and accelerograms representing excitations at bedrock level are available in the digitised form. Thus, accelerograms that were recorded on rock sites are particularly valuable for structural design practices.

Recorded accelerograms are mostly sourced from a tectonically active area where earthquakes are well known (eg. Western North America, Taiwan and the Middle East), and only a small number of accelerograms were recorded on rock (which can be used as input into program *SHAKE* for obtaining site specific ground motions). Thus, one need to resort to the use of artificial accelerograms as a supplement to recorded accelerograms. Artificial accelerograms representing bedrock conditions may be derived from *ground motion prediction expressions* (GMPE) using software such as *Seismo-Artif* which is for open access via the internet but such expressions are mostly derived from tectonically active areas where strong motion records are in abundance for developing empirically based GMPEs.

Another approach of generating accelerograms by the com*p*uter is through the use of band-limited random signals to represent seismic waves radiated from the source of the earthquake along with modifications of the frequency contents of the radiated waves along their travel path. The methodology as described for simulating ground motions is known as stochastic simulations. The frequency content of the simulated accelerograms is controlled by the seismological model. This paper is mainly concerned with stochastic simulations of the seismological model for the generation of accelerograms (Boore & Joyner, 1991; Joshi et al. 1999; Lam, et al. 2000; Rezaeian & Kiureghian, 2010). Many Ground motion models that have been developed for tectonically stable areas are based on this methodology.

More recently, non-parametric models have been developed from recorded ground motions based on the European database (Zentner & Poirion, 2012). The wavelet packet approach has also been adopted for constructing artificial accelerograms (Yamamoto & Baker, 2013).

The translation of a seismological model for simulating accelerograms, or for the development of a GMPE, requires a computer software such as *SMSIM* (Boore, 2000) or *GENQKE* (Lam, et al. 2000) for undertaking the simulations. A proper use of such simulation software requires a good understanding of stochastic simulations and the

seismological models in order to avoid misuse of the software. The authors favour publishing guidance on how to simulate accelerograms on a generic analytical platform such as *MATLAB,* or *EXCEL,* to assist designers and fellow researchers as opposed to offering the program (*GENQKE*) as a "black box" tool. An important aim of this paper is to accomplish this (Section 2). A summary listing of a few well known seismological models is then presented to inform the users (Section 3). Simulated accelerograms based on the seismological model of Atkinson and Boore (1995) which is abbreviated herein as AB95 have been employed in PSHA for the prediction of seismic hazard for a low seismicity area. Predictions from AB95 through PSHA of a low seismicity environment are compared with predictions from other ground motion models developed for *Eastern North America* (ENA) and the 2nd edition of the *Next Generation Attenuation Expressions* for *Western North America,* NGA-West2 (Section 4).

2. Generation of Synthetic Accelerograms

Program *GENQKE* which was originally written by the second author for introducing the idea of stochastic simulations of the seismological model (for the generation of synthetic accelerograms) has been around for 20 years. The program has contributed to research and consulting activities both within Australia and internationally. The original program was written in the old *Fortran* 99 language. It is intention of the authors to encourage fellow researchers, and engineers to re-write the program in a contemporary, commonly used, platform that can be shared around amongst professional engineers readily, like *MATLAB, Visual Basic* or *EXCEL*. In many ways it is beneficial to have the program algorithm made transparent in order to have its potentials and limitations well understood by the users in order that it will no longer be a “black box”. The program can also be customised in its further development to suit specific needs. This section is aimed at explaining the basic construction of program *GENQKE* in order that any researcher who has had experience with programming would be able to rewrite the program in one's preferred computational platform. Essentially, the generation of synthetic accelerograms in accordance with a seismological model involves the following steps:

(Step 1) **Generation of *Gaussian* White Noise *nt(t)*** - *Gaussian* white noise can be generated by a random number generator that has been built into the computer and can be accessed from many platforms including *MATLAB* and *EXCEL*. The white noise has to be band-limited in between the lowest frequency value *df (*which is reciprocal of the duration of the simulated time-history) and the highest frequency *(N/2-1) df* where *N* is the number of time-steps in the simulation. Refer Figure 1 for a schematic illustration.

(Step 2) **Time windowing of *Gaussian* White Noise *st(t)*** - A window function *win*(*t*) is then applied to modulate the signal in the time domain (Fig. 1).

Essentially,

$$st(t) = win(t) * nt(t) \tag{1a}$$

where *nt*(*t*) is the band-limited *Gaussian* white noise prior to the imposition of windowing ; *win(*t) is the imposed time window function which has been scaled in such a way not to alter the overall amplitude of the *Gaussian* white noise. The windowing function *win(t)* can be of the *trapezoidal* or *exponential* form. The latter has been adopted in this study and is defined by equation (1b).

$$win(t) = e^{0.4t(6/t_d)} - e^{-1.2t(6/t_d)} \quad (1b)$$

where

$$t_d = \frac{1}{f_0} + bR \quad (1c)$$

f_0 *is corner frequency, R is hypocentral distance, and b is a constant. st(t)* is the windowed white noise and there is an ensemble of such white noise time series with random variability between them.

(Step 3) ***Fourier T*ransform of Windowed White Noise *As(f)*** - Both *MATLAB and EXCEL* has built-in capabilities to handle *Fourier* Transform *of the windowed white noise* for calculating their *Fourier* Amplitude values which have random variability in between simulations and is averaged to unity across the simulated accelerogram ensemble. The set of phase angles obtained from the *Fourier* Transform is reserved for use in Step 6.

(Step 4) **Identifying a suitable seismological model *Ax(f)* -** The seismological model is essentially the frequency filter *Ax(f)* which defines the frequency content of the ground motion in the form of a Target *Fourier* Amplitude Spectrum as illustrated in Figure 1. A summary listing of the well-publicized, and established, seismological models is presented in Section 3. An introduction to the concept of seismological modelling can also be found in the review article by Lam *et al.* (2000).

(Step 5) **Filtering windowed white noise by the seismological model *Aa(f)* -** *Fourier* Amplitude Spectrum ***Aa(f)*** is essentially product of ***As(f)*** obtained from Step 3 and ***Ax(f)*** from Step 4. ***Aa(f)*** of an individual simulation can have considerable random variability. Importantly, the ensemble averaged ***Aa(f)*** as derived from repetitive simulations should display convergence to ***Ax(f)*** (Figure 2).

(Step 6) **Inverse *Fourier* Transform of the *windowed-filtered white noise* for generating synthetic accelerograms *a*(*t*) –** Inverse *Fourier* Transform of ***Aa(f)*** as obtained from Step 5 whilst incorporating the phase angles obtained from Step 3 to give the ground motion time-series ***a*(*t*).** Refer Figure 3a – 3c for a typical sample of the simulated time series which are presented in the form of the acceleration, velocity and displacement formats.

The procedure of generating synthetic accelerograms is illustrated holistically in Figure 1.

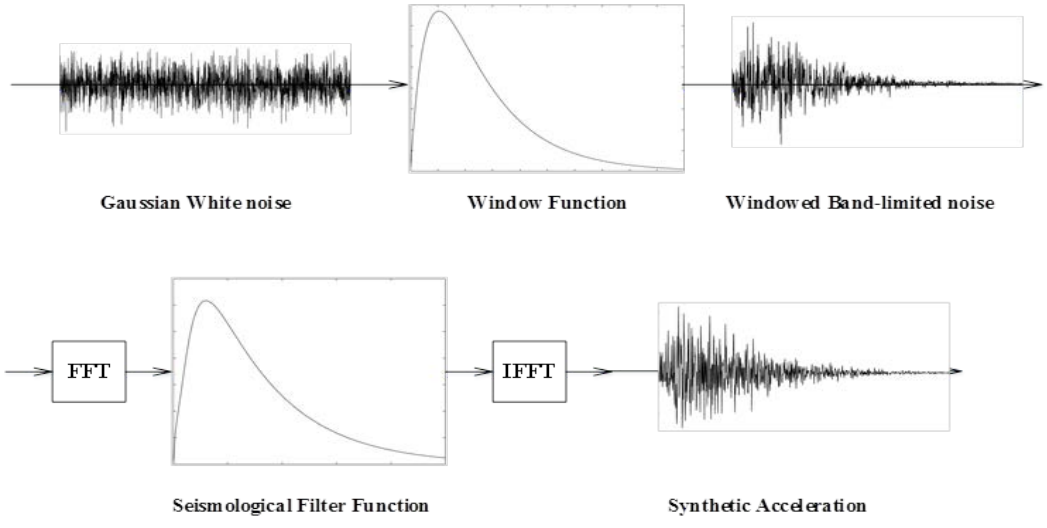

Figure 1. Procedure for generating a synthetic acceleration time history

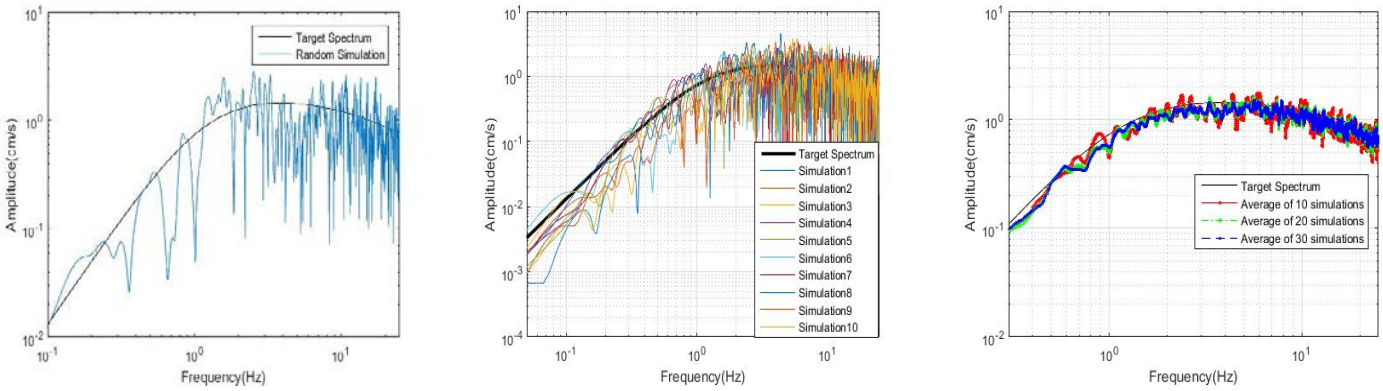

(a) Single random simulation (b)10 random simulations (c)average of random simulation

Figure 2. Simulated Fourier Spectra vs The Target Spectrum

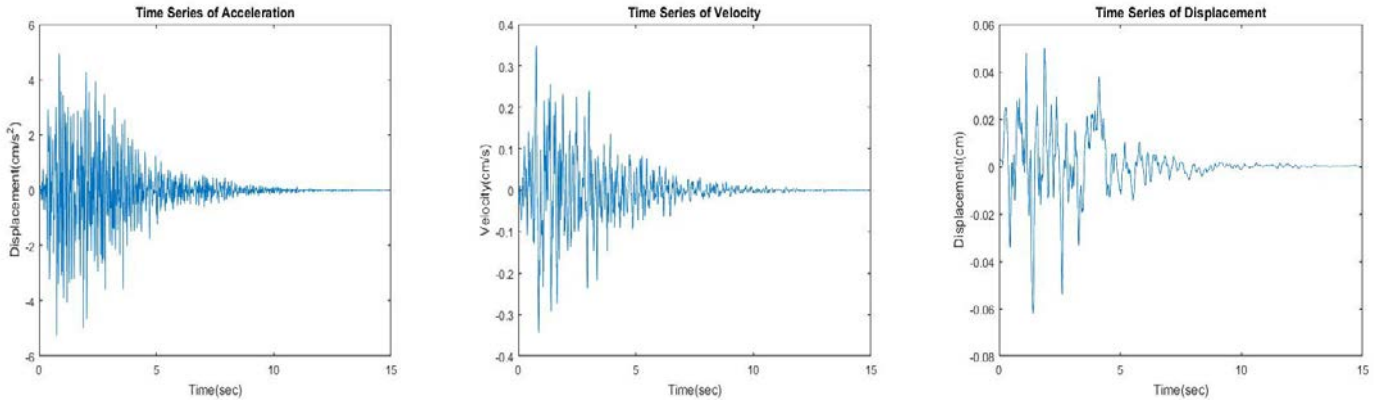

(a) Acceleration (b) Velocity (c) Displacement

Figure 3. Simulated Ground Motion Time Histories

3. Listing of the Seismological Models

The seismological model is made up of several component factors namely the source factor and various attenuation and amplification factors and can be expressed in the form of equation (2).

$$\mathrm{E}(M_0, R, f) = S(M_0, f) * G(R) * An(f, R) * P(f) * I(f)^n \qquad (2)$$

Where:

$E(M_0, R, f)$ is the target *Fourier* spectrum;

$S(M_0, f)$ is the source factor*;*

$G(R)$ is the geometric attenuation factor*;*

$An(f, R)$ is the anelastic whole path attenuation factor*;*

$P(f)$ is the upper crust attenuation factor*;*

$I(f) = 2\pi f$, which is the shape factor; for $n = 0$, $\mathrm{E}(M_0, R, f)$ represents the target *Fourier* spectrum for acceleration*;* for $n = -1$, $\mathrm{E}(M_0, R, f)$ is for velocity*;* and for $n = -2$, $\mathrm{E}(M_0, R, f)$ is for displacement.

M_0 is defined as the seismic moment in units of *dyne-cm; f* is the frequency of the ground motion in *Hz; R* is distance between the source and the site in units of *km.*

3.1 Source factors

Source factors that have been developed to date based on the notion of a "point source" have been reported in the literature (Atkinson & Boore, 1995; Atkinson, 2004; Atkinson & Boore, 2014;Boore, 1983; Brune, 1970). A *Point Source Model* considers the source of an earthquake as a point from which seismic waves are radiated. If the source of earthquake is large enough that cannot be regarded as a "point", the point source model cannot be adopted any more, that's why some researchers put forward the finite fault source model. In contrast, a *Finite fault model* considers the earthquake generating source to be made up of a large number of sub-faults each of which can be treated as a point source (Tumarkin & Archuleta, 1994; Zeng, et al. 1994; Miyake, et al. 2003; Motazedian & Atkinson, 2005)**.**

The most commonly accepted source model of the acceleration *Fourier Spectrum* is represented by the *single-corner frequency* source factor of Brune (1970) which is defined by equation (3).

$$\mathrm{S}(M_0, f) = (2\pi f)^2 \frac{CM_0}{(1+(f/f_0)^2)} \tag{3}$$

In which, *C* is the mid-crust scaling factor as defined by equation 4 (Atkinson, 1993).

$$\mathrm{C} = \frac{R_p FV}{4\pi\rho\beta^3 R_0} \tag{4}$$

where $R_0 = 1$km; R_p is the average radiation pattern (=0.55); F is the free surface amplification factor (=2.0); V is the partitioning factor of the two horizontal components (=0.71); ρ is crustal density; and β is shear wave velocity.

Seismic moment M_0 can be expressed in terms of the moment magnitude which is given by equation 5(Hanks & Kanamori, 1979):

$$M = 0.67 \log(M_0) - 10.7 \tag{5}$$

f_0 is corner frequency as defined by equation (6) as per the model developed by Brune (1970).

$$f_0 = 4.9 \times 10^6 \beta \left(\frac{\Delta\sigma}{M_0}\right)^{1/3} \tag{6}$$

where β is shear wave velocity in *km/s*, and $\Delta\sigma$ is stress drop in *bars.*

For large magnitude (M >6) earthquakes the observed *Fourier* spectrum is better modelled by the *double corner frequency* source factor which was introduced by Atkinson & Boore (1995). The basic form of the source factor is defined by equation (7).

$$S(M_0, f) = (2\pi f)^2 C M_0 \left[\frac{1-\varepsilon}{1+(f/f_A)^2} + \frac{\varepsilon}{1+(f/f_B)^2}\right] \tag{7}$$

In which parameters in the model are functions of moment magnitude within the range: *(*$4 \leq M \leq 7$*)* as defined by equations. 8a – 8c*:*

$$log\varepsilon = 2.52 - 0.637M \quad (8a)$$

$$logf_A = 2.41 - 0.533M \quad (8b)$$

$$logf_B = 1.43 - 0.188M \quad (8c)$$

Figure 4 shows the comparison of the Fourier Spectrum as obtained from the *single corner frequency* model and the *double corner frequency* model (*R*=1km).

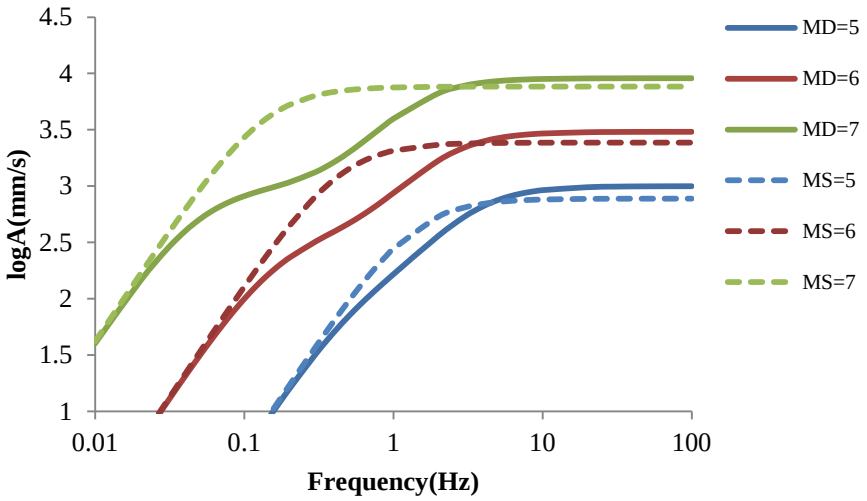

Figure 4. Comparison of source spectrum derived from Double Frequency Model and Single Frequency Model ($\Delta\sigma = 100$bar) for M $= 5, 6, 7$

3.2 Geometric attenuation factors

The geometric attenuation factors are of profound significance in ground motion modelling. Several geometric attenuation relationships have been proposed in the literature (refer Table 1 and Figure 5)

Table 1. Summary of Geometric Attenuation models (Report, 2015)

Geometric spreading functions	"R"	Applicable range	Model and Reference
$R \le 70, G(R) = R^{-1}$; $70 \le R \le 130, G(R) = 70^{-1} * (\frac{R}{70})^{0}$; $R > 130, G(R) = 70^{-1} * 130^{0} * (\frac{R}{130})^{-0.5}$	$R = R_{hyp}$	$4 \le M \le 7.25$ $10 \le R \le 500$ $0.5 \le f \le 20$	AB95 (Atkinson & Boore, 1995)
$R \le 80, G(R) = R^{-(1.0296-0.0422(M-6.5))}$ $R > 80, G(R) = 80^{-(1.0296-0.0422(M-6.5))} * R^{-0.5*(1.0296-0.0422(M-6.5))}$	$R = R_{hyp}$	$4.5 \le M \le 8.5$ $1 \le R \le 400$ $0.1 \le f \le 100$	SGD02 (Walter, et al.2002)
$R \le 70, G(R) = R^{-1.3}$; $70 \le R \le 140, G(R) = 70^{-1.3} * (\frac{R}{70})^{0.2}$; $R > 140, G(R) = 70^{-1} * 140^{0.2} * (\frac{R}{140})^{-0.5}$	$R = R_{hyp}$	$4.4 \le M \le 6.8$ $10 \le R \le 800$ $0.05 \le f \le 20$	A04 (Atkinson, 2004)
$G(R) = R^{-1}$, *for all* R	$R = (R_{hyp}{}^2 + h_{FF}{}^2)^{0.5}$, $h_{FF} = 10^{-00405+0.235M}$	$4.4 \le M \le 6.8$ $10 \le R \le 800$ $0.05 \le f \le 20$	BCA10d (Boore, et al. 2010)
$R \le 50, G(R) = R^{-1}$; $R > 50, G(R) = 50^{-1} * (\frac{R}{50})^{-0.5}$	$R = R_{hyp}$	$4.4 \le M \le 5.0$ $23 \le R \le 602$ $0.2 \le f \le 20$	BS11 (Boatwright & Seekins, 2011)
$R \le 50, G(R) = 10^{T_C C_{LF}} R^{-1.3}$; $R > 50, G(R) = 50^{-1.3} * (\frac{R}{50})^{-0.5}$ $f \le 1, T_C = 1$; $1 < f < 5, T_C = 1 - 1.429 \log(f)$; $f \ge 5, T_C = 0.$ $R \le h, C_{LF} = 0.2 \cos((\pi/2)(R-h)/(1-h))$; $10 < R < 50, C_{LF} = 0.2 \cos\big(((\pi/2)(R-h)/(1-h))\big)$;	$R = (R_{hyp}{}^2 + h_{FF}{}^2)^{0.5}$, $h_{FF} = 10^{-00405+0.235M}$ h = focal depth	$3.5 \le M \le 6.0$ $10 \le R \le 500$ $0.2 \le f \le 20$	AB14 (Atkinson & Boore, 2014)

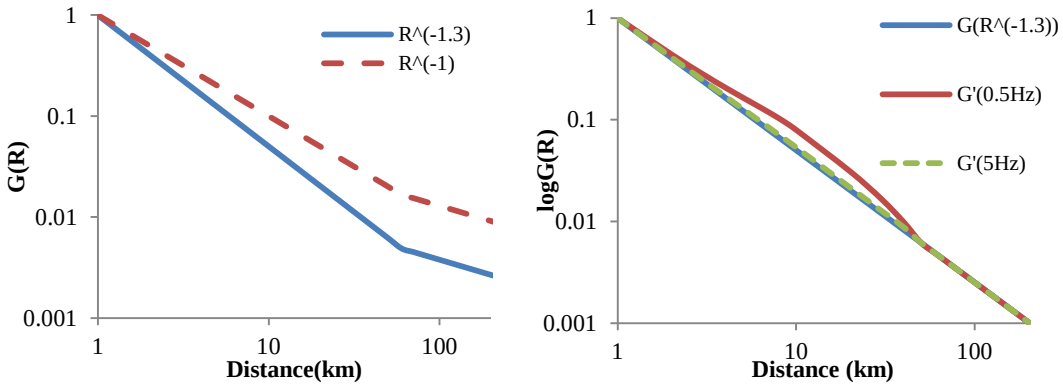

Figure 5. Comparison of geometric spreading functions

3.3 Anelastic whole path attenuation factor

The *anelastic whole path attenuation factor* is to account for energy dissipation along the wave travel path and is to be distinguished from the *geometrical* factor. The *anelastic attenuation factor* can be expressed in the form of eqn. (9).

$$An(f,R) = exp(-\pi f R/Q\beta) \tag{9}$$

where Q is the *Quality Factor*.

Functions that have been proposed for quantifying the frequency dependence of Q are summarized in Table 2 and Figure 6.

Table 2. Summary of Anelastic Attenuation Models

"Q"	**Applicable range**	**Model and Reference**
$Q(f) = 680f^{0.36}$	$4 \le M \le 7.25$ $10 \le R \le 500$ $0.5 \le f \le 20$	AB95 (Atkinson & Boore, 1995)
$Q(f) = 351f^{0.84}$	$1 \le R \le 400$ $0.1 \le f \le 100$	SGD02 (Walter et al., 2002)
$Q(f) = max(1000, 893f^{0.32})$	$4.4 \le M \le 6.8$ $10 \le R \le 800$ $0.05 \le f \le 20$	A04 (Atkinson, 2004)
$Q(f) = 2850$	$4.4 \le M \le 6.8$ $10 \le R \le 800$ $0.05 \le f \le 20$	BCA10d (Boore et al., 2010)
$Q(f) = 410f^{0.5}$	$4.4 \le M \le 5.0$ $23 \le R \le 602$ $0.2 \le f \le 20$	BS11 (Boatwright & Seekins, 2011)
$Q(f) = 525f^{0.45}$	$3.5 \le M \le 6.0$ $10 \le R \le 500$ $0.2 \le f \le 20$	AB14 (Atkinson & Boore, 2014)

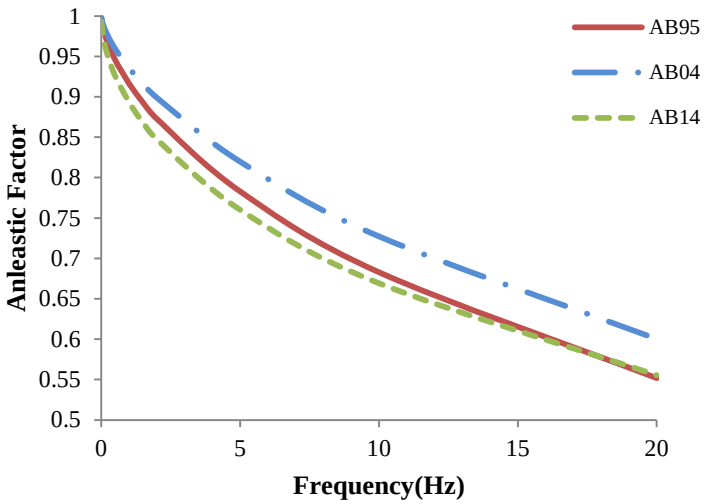

Figure 6. Samples of anelastic attenuation functions

3.4 Upper crustal attenuation factor

There are two basic forms of the upper crustal attenuation factor *P(f)*.

$$P(f) = [1 + (f/f_m)^8]^{-1/2} \quad (10a)$$

or

$$P(f) = \exp(-\pi k f) \quad (10b)$$

where f_m is the high frequency cut-off factor. In *Eastern North America* (ENA), 50 Hz is often assumed as the cut-off frequency; k is the rate of high-frequency decay as shown on graphs of *log spectra* versus *frequency* which is a high-cut filter for use in modelling near-surface phenomena (Anderson & Hough, 1984). Refer Figure 7.

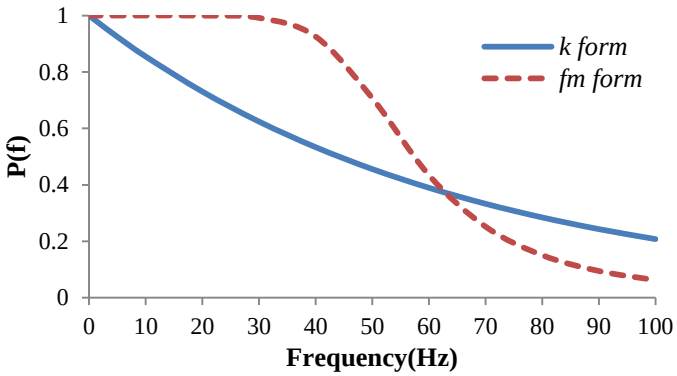

Figure 7. Samples of upper-crust attenuation functions

4. Incorporating a Seismological Model into Probabilistic Seismic Hazard Analysis

The mainstream methodology that has been adopted for deriving ground motion models for *Next Generation Attenuation Relationships* for *Eastern North America* (NGA-East) is stochastic simulation of the seismological model. In the evaluation work of Boore (Chapter 2 in PEER 2015/04) the point source simulation models of Atkinson and Boore (1995), Boatwright and Seekins (2011) and Boore *et al.* (2010) (abbreviated herein as AB95, BS11 and BCA10d respectively) have been considered

by the review to be very consistent with data recorded in the field. An independently developed GMM (*DASG15*) as introduced in Chapter 3 of PEER 2015/04 has also been constructed from a seismological model that had been derived (more recently) from the broadband inversion of the NGA-East database. Other models from reputable sources including the hybrid empirical models (*PZCT15*), the Central and Eastern North America (CENA) finite fault models (e.g. *SP15*), and the traditional empirical model of *ANC15* that were derived from macro-seismicity data (that are introduced in Chapters 5, 7 and 8 of PEER 2015/04) have also been included in this investigatory study.

Table 3 A selection of ground motion models for use in tectonically stable regions

Literature citations	Acronyms in legends	Remarks
Atkinson and Boore (1995)	AB95	BSSA article 2014
Pezeshk, Zandieh, Campbell and Tavakoli (2015)	PZCT15	PEER report 2015/04
Darragh *et al*. (PEER, 2015)	DASG15	PEER report 2015/04
Shahjouei and Pezeskh (PEER, 2015)	SP15	PEER report 2015/04
Al Noman and Cramer (PEER, 2015)	ANC15	PEER report 2015/04
Silva, Gregor and Darragh (2002)	SGD02	PEA report 2002
Atkinson (2004)	A04	BSSA article 2014
Boore, Campbell and Atkinson (2010)	BCA10d	BSSA article 2014
Boatwright and Seekins (2011)	BS11	BSSA article 2014
Atkinson and Boore (2014)	AB14	BSSA article 2014

Results of PSHA showing *RSA* values at 0.3 s and 1.0 s based on a selection of GMMs of *NGA-East* are superposed on the range of predictions based on the GMMs of *NGA-West2* (Figures 8a – 8b). Ground motion models namely *AB95* and *DASG15* are more robust than the *SP15* and *PZCT15* models in terms of inter-model consistencies. An earlier independent review of GMMs developed for use in ENA by Ogweno and Cramer (2014) also ranked *AB95* favourably in view of consistencies between the model predictions and field recordings. There is no intention to identify which GMMs are the more "correct" GMM for CENA. It so happens that predictions from the *AB95* and the *DASG15* GMMs of *NGA-East* are overall comparable with predictions from the *NGA-West2* and only marginally higher at 0.3s.

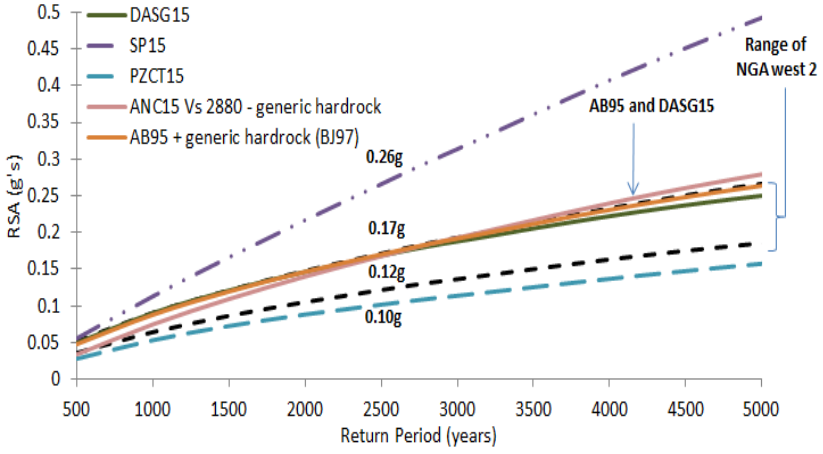

(a) 0.3s period

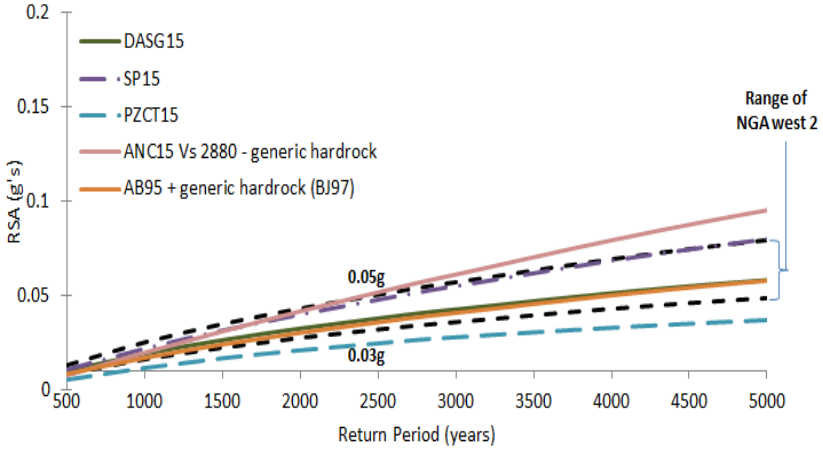

(b) 1.0s period

Figure 8. Results of PSHA on rock for Log10N = 5.5-0.9M (i.e., KD = 2) for NGA-East Mmin = 5 and Mmax = 7 (response spectral values are based on 5% viscous damping)

It is cautioned herein that ground motion models listed in Table 3 and plotted in Figure 8 are based on intraplate cratonic crustal environment (which is characteristic of ENA). Ground motion predictions for intraplate non-cratonic crustal environment are beyond the scope of this paper.

5. Conclusion

The computation algorithm for the stochastic simulations of the seismological model for the generation of synthetic accelerograms was first presented with the aim of enabling readers to perform simulations on *MATLAB* or *EXCEL*. A summary listing of a few established seismological models was then presented. The source factor along with various attenuation and amplification factors which constitute the seismological model were then introduced under separate sub-headings. Finally, a few ground motion models that have been developed for use in *Eastern North America* were compared and benchmarked against the *Next Generation Attenuation Relationships* for *Western North America* (NGA – West2) in the form of results from *probabilistic seismic hazard analysis* (PSHA). Models that are relatively more robust and give predictions that are in good agreement with other models have been identified. Ground motion predictions for intraplate non-cratonic environment are outside the scope of the paper.

Acknowledgements

We have benefited from the Ground Motion Databases (http://www.seismotoolbox.ca/GMDatabases.html). The support of the Commonwealth of Australia through the Cooperative Research Centre program is also acknowledged.

References

Al Atik, L., & Youngs, R. R. (2014). Epistemic uncertainty for NGA-West2 models. Earthq. Spectra, Vol 30, pp 1301-1318.

Anderson, J., & Hough, S. (1984). A model for the shape of the Fourier amplitude spectrum of acceleration at high frequencies. Bull. Seism. Soc. Am, Vol 74, pp 1969-1993.

Atkinson, G. (1993). Earthquake Source Spectra in Eastern North America. Bull. Seism. Soc. Am, Vol 83, No. 6, pp 1778-1798.

Atkinson, G., & Boore, D. (1995). Ground-Motion Relations for Eastern North America. Bull. Seism. Soc. Am, Vol 85, pp 17-30.

Atkinson, G. (2010). Ground-motion prediction equations for Hawaii from a referenced empirical approach. Bull. Seism. Soc. Am, Vol 101, pp 1304-1318.

Atkinson, G. (2004). Empirical attenuation of ground-motion spectral amplitudes in southeastern Canada and the northeastern United States. Bull. Seism. Soc. Am, Vol 94, pp 1079-1095.

Atkinson, G., & Boore, D. (2014). The attenuation of Fourier amplitudes for rock sites in eastern North America. Bull. Seism. Soc. Am, Vol 104, pp 513-528.

Boatwright, J., & Seekins, L. (2011). Regional spectral analysis of three moderate earthquakes in northeastern North America. Bull. Seism. Soc. Am, Vol 101, pp 1769-1782.

Boore, D. (1983). Stochastic simulation of high-frequency ground motions based on seismological models of the radiated spectra. Bull. Seism. Soc. Am, Vol 73, pp 1865-1894.

Boore, D., & Joyner, W. B. (1991). Estimation of ground motion at deep soil sites in Eastern-north America. Bull. Seism. Soc. Am, Vol 81, pp 2167-2185.

Boore, D., Campbell, K. W., & Atkinson, G. (2010). Determination of stress parameters for eight well-recorded earthquakes in eastern North America. Bull. Seism. Soc. Am, Vol 100, pp 1632-1645.

Bora, S. S., Scherbaum, F., Kuehn, N., et al. (2015). Development of a Response Spectral Ground-Motion Prediction Equation(GMPE) for Seismic-Hazard Analysis from Empirical Fourier Spectral and Duration Models. Bull. Seism. Soc. Am, Vol 105, pp 2192-2218.

Boore, D., Stewart, J., Seyhan, E. and Atkinson, G. (2014). NGA-West2 equations for predicting PGA, PGV, and 5% damped PSA for shallow crustal earthquakes. Earthq. Spectra, Vol 30, No 3, pp 1057-1085

Brune, J. N. (1970). Tectonic stress and the spectra of seismic shear waves from earthquakes. J. Geophys .Res, Vol 75, pp 4997-5009.

Hanks, T. C., & Kanamori, H. (1979). A moment magnitude scale. J. Geophys .Res, Vol 84, No B5, pp 2348-2350.

Joshi, A., Kumar, B., Sinvhal, A., & H.Sinvhal. (1999). Generation of synthetic accelerograms by modeling of rupture plane. Journal of Earthquake Technology, Vol 36 No 1, pp 43-60.

Lam, N., Wilson, J., & Hutchinson, G. (2000). Generation of Synthetic Earthquake Accelerogram Using Seismological Modelling: A Review. Journal of Earthquake Engineering, Vol 4, No 3, pp 321-354.

Miyake, H., Iwata, T., & Irikura, K. (2003). Source characterization for broadband ground-motion simulation: Kinematic heterogeneous source model and strong motion generation area. Bull. Seism. Soc. Am, Vol 93 No 6, pp 2531-2545.

Motazedian, D., & Atkinson, G.(2005). Stochastic Finite-Fault Modelling Based on a Dynamic Corner Frequency. Bull. Seism. Soc. Am, Vol 95, pp 995-1010.

Ogweno, L. and Cramer, C. (2014). Comparing the CENA GMPEs Using NGA-East Ground Motion Database. Seismol. Res. Lett., Vol 85, No 6, pp 1377-1393.

Report, (2015). NGA-East: Median Ground-Motion Models for the Central and Eastern North America Region. PEER.

Rezaeian, S., & Kiureghian, A. D. (2010). Simulation of synthetic ground motions for specified earthquake and site characteristics. Earthquake Engineering and Structural dynamics, Vol 39, pp 1155-1180

Tumarkin, A., & Archuleta, R. (1994). Empirical ground motion prediction. Ann. Geofis., Vol 37, pp 1691-1720.

Walter, S., Nick, G., & Robert, D. (2002). Development of regional hard rock attenuation relations for central and eastern north America. Report to Pacific Engineering and Analysis.

Yamamoto, Y., & Baker, J. W. (2013). Stochastic Model for earthquake ground motion using wavelet packets. Bull. Seism. Soc. Am, Vol 103 No 6, pp 3044-3056.

Zeng, Y., Anderson, J., & Yu, G. (1994). A composite source model for computing realistic synthetic strong ground motions. Geophys. Res. Lett., Vol 21, pp 725-728.

Zentner, I., Allain, F., Humbert, N., & Caudron, M. (2014). Generation of spectrum compatible ground motion and it's use in regulatory and performance-based seismic analysis. Proceedings of the 9th International Conference on Structural Dynamics, EURODYN,2014, pp 381-386.

Zentner, I., & Poirion, F. (2012). Enrichment of seismic ground motion database using Karhunen-Loeve expansion. Earthquake Engineering and Structural dynamics, Vol 41, No 14, pp 1945-1957.